Hindawi
Mathematical Problems in Engineering
Volume 2019, Article ID 4634131, 12 pages
https://doi.org/10.1155/2019/4634131

Research Article

The Integration of Wind-Solar-Hydropower Generation in Enabling Economic Robust Dispatch

Peng Wei[1] **and Yang Liu**[2]

[1] *Yalong River Hydropower Development Company Ltd., Chengdu 610000, China*
[2] *College of Electrical Engineering and Information Technology, Sichuan University, Chengdu 610065, China*

Correspondence should be addressed to Yang Liu; yang.liu@scu.edu.cn

Received 6 August 2018; Revised 3 December 2018; Accepted 17 December 2018; Published 2 January 2019

Academic Editor: Alessandro Mauro

Currently the renewable energies including wind power and photovoltaic power have been increasingly deployed in power system to achieve contamination free and environmental-friendly power production. However, due to the natural characteristics of wind and solar, both wind power and photovoltaic power contain uncertainty and randomness which may significantly impact the stability, security, and economic efficiency of the conventional power system mainly consisted by hydropower and thermal power. To deal with the issue, this paper presents a two-stage robust model which is able to achieve the optimal day-ahead dispatch strategy in the worst-case scenario of wind and photovoltaic outputs. Because of the strong interactions between the two stages, the original optimization has been decomposed into the day-ahead dispatch master problem and the additional adjustment subproblem considering the uncertainty and randomness of the wind and the photovoltaic outputs. Also, the piecewise linearization technique is employed to convert the original problem into a MILP problem. Afterward, the dualization of the additional adjustment subproblem can be obtained by using linear programming strong duality theory. Additionally, the Big-*M* method enables the linearization of the dual model. The interacted-iterations between the master problem and the subproblem are successfully implemented which can ultimately figure out the optimal day-ahead dispatch strategy of the power system with conventional and renewable energies.

1. Introduction

To achieve the contamination free and environmental-friendly power generation, clean energies such as wind power generation and photovoltaic power generation have been increasingly deployed in modern power systems [1]. It has been widely admitted that such renewable energies can effectively deal with the increase of the power consumption with less environmental impacts. However, it is also realized that the uncertainty and randomness of the wind and photovoltaic power generations are extremely difficult to be predicted. Therefore, the security and the economical-efficiency including voltage, frequency, and power loss of the conventional power system may be severely affected with high penetration of the wind and photovoltaic power generations. As one of the conventional power generations in power system, hydropower is regarded as a kind of energy source with highly flexible adjustment ability, which has remarkable potential to effectively handle the uncertainty and randomness of the wind and photovoltaic power generations. By coordinating the hydropower, accommodation capability of serving the wind power and photovoltaic power can be significantly improved [2]. Therefore this paper combines the wind power, photovoltaic power, hydropower, and thermal power for coscheduling. Additionally, it should be pointed out that the integration of multiple energy sources may also greatly improve the operating efficiency of power system [3, 4]. Research [3] presents a new mathematical model for the simulation of solid oxide fuel cell based on the combined heat and power system, in which the cogeneration units have high operating efficiency. Research [4] presents a novel poly-generation system, including cogenerative proton exchange membrane fuel cell, concentrated photovoltaic-thermal collectors, and so on. The experimental result shows that the total electrical and thermal efficiencies remain high. It can be seen that the integration of multiple energy sources

is economically viable. Quite a few researches [5–26] also focus on the integration of the multiple energies in the power system, and also they point out that the optimal dispatch strategy for the coordination of the energies becomes highly important.

To study the integration of the clean energies, researches [5–7] mainly aim at improving the system reliability and flexibility using the optimal coordination of wind power, photovoltaic power, and hydropower. However, they have not considered the uncertainty and randomness of the wind power and the photovoltaic power which may lead to errors in their researches. The deterministic programming and stochastic programming are the common approaches to handle the uncertainties of the renewable energy sources [8]. Researches [9, 10] add the spinning reserve into the deterministic dispatch model. Although their approach improves the system security, it simultaneously limits the economy and the flexibility of the system. Researches [11, 12] establish the uncertainty dispatch models based on the probability distributions, for example, Weibull and Beta distributions. However, it should be realized that these two hypothetical distributions cannot accurately describe the behaviors of wind and solar so that the deviations certainly occur between their dispatch model and the practical requirements. Researches [13, 14] mainly employ the multiscenario approach to convert the stochastic optimization problem into the deterministic problem. The multiscenario approach trades off the scenario reduction in terms of computing efficiency. In the scenario reduction operations, certain extreme scenarios may be lost resulting in the inaccuracy of the optimization [15]. Recently, robust optimization has been widely employed in the economical dispatch as it needs neither precisely modeled probability distribution nor large-scale sampling of uncertain variables [16–18]. Research [16] presents a static robust optimization model to deal with the uncertainties. However, the static robust optimization tends to be overconservative. Thus, researches [17, 18] further present the two-stage robust optimization model with the "min-max-min" structure. Additionally, an adjustable robust parameter is introduced to control the conservatism of the scheme. Based on their studies, the original problem can be decomposed into the master problem and the subproblem based on the type of decision variables.

Due to the uncertainty in the renewable energy sources, the adjustment between the base generation and the actual generation should be considered. Researches [19–21] place emphasis on the acquisition of adjustment strategy for unbalanced power caused by the prediction error. Research [19] introduces the multiagent technology in the microgrid to formulate the energy scheduling strategy. Research [20] presents a method that considers variability and uncertainty cost of renewable energy sources between two consecutive scheduling intervals in the real-time. Research [21] further links up the day-ahead scheduling and real-time scheduling by a more meticulous generation dispatch mode to formulate a comprehensive strategy. Researches [22–26] introduce the market mechanism to ensure the economic efficiency of power system considering the risk due to uncertainties. The overestimation and underestimation costs of the renewable energy sources are considered in the objective, which is similar to the upregulation and downregulation in the adjustment stage.

Motivated by the previous works, this paper presents a two-stage robust model considering the generation of wind power, photovoltaic power and hydropower in enabling the day-ahead economical dispatch strategy for power system. In our model the fluctuations of wind output and photovoltaic output caused by the randomness and uncertainty are evened out using hydropower and thermal power. Especially due to the strong adjusting ability of hydropower, the model deals with the fluctuations prioritizing the hydropower and then the thermal power because of its feeblish adjusting ability. Additionally, to improve the wind and photovoltaic power accommodation capability of the power system, this paper regards the wind power and photovoltaic power curtailment costs as penalty function in the presented model. This paper also linearizes the original two-stage robust problem and then employs the strong duality theory to handle the max-min subproblems. At last the ultimate optimal solution can be achieved using the model decomposition and iterations. The effectiveness of the presented approach has been evaluated using the IEEE-30 bus system.

The rest of the paper is organized as: Section 2 presents the day-ahead dispatch robust model considering the wind power, photovoltaic power, and hydropower; Section 3 presents the linearization of the model; Section 3 solves the preprocessed two-stage model; Section 4 evaluates the approach and discusses the simulation results; Section 5 concludes the paper.

2. Day-Ahead Dispatch Robust Model Considering Wind Power, Photovoltaic Power, and Hydropower

2.1. The Details of the Two-Stage Robust Model. Modern power systems contain not only thermal power and hydropower but also wind power and photovoltaic power. In this section, the optimal dispatch model is presented for a power system with thermal power and renewable energies including wind, photovoltaic, and hydropower. At the very beginning of the modeling, without considering the uncertainty and randomness of the wind and photovoltaic power, the day-ahead dispatch strategy is an optimization problem based on the identification of the minimum operating cost, which is represented by

$$\begin{aligned} \min_{x} \quad & C_{\text{ope}}(x) \\ \text{s.t.} \quad & A_{\text{ope}}(x) = 0, \\ & B_{\text{ope}}(x) \le 0 \end{aligned} \tag{1}$$

where $C_{\text{ope}}(\cdot)$ is the conventional day-ahead operating cost of the power system, which is mainly the cost of the thermal power; x is the day-ahead dispatch scheme including the status and the outputs of the thermal units and the hydropower units; $A_{\text{ope}}(\cdot)$ and $B_{\text{ope}}(\cdot)$ represent the day-ahead equality constraint and the inequality constraint representing the

power balance constraint, branch power flow constraints, thermal power units constraints, hydropower unit constraint, wind and photovoltaic outputs constraints, and so on.

In (1), the outputs of the wind and photovoltaic generation are based on the prediction. However, precise prediction of the outputs is difficult so that the power imbalance in the system certainly occurs [27]. The imbalance can be compensated by using additional adjustments which can be regarded as a second stage problem named as additional adjustment stage. As a result, in our model, the outer layer is a max problem which is adopted to identify the worst-case scenario (the scenario under which the adjustment cost is the highest) with the x based uncertain parameters. The inner layer is a min problem which is adopted to figure out the minimum additional adjustment costs under the worst-case scenario. The overview of the model is represented by

$$\begin{aligned} \max_{u\in U}\ \min_{y\in\Omega(x,u)} \quad & C^{+}_{\mathrm{ope}}(u,y) \\ \text{s.t.} \quad & A^{+}_{\mathrm{ope}}(y)=0, \\ & B^{+}_{\mathrm{ope}}(y)\le 0 \end{aligned} \tag{2}$$

where $C^{+}_{\mathrm{ope}}(\cdot)$ is the additional adjustment costs based on the day-ahead dispatch scheme x; $C^{+}_{\mathrm{ope}}(\cdot)$ is mainly consisted of units adjustment cost, wind power and photovoltaic power curtailment costs; u is the uncertain parameters; U is the feasibility region of u; y is the adjustment scheme which is able to handle the uncertainty; $\Omega(\cdot)$ is the feasibility region based on certain known values (e.g., $y\in\Omega(x,u)$ means that feasibility region of y is constrained by x and u that have been optimized); $A^{+}_{\mathrm{ope}}(\cdot)$ and $B^{+}_{\mathrm{ope}}(\cdot)$ represent the power balance constraint, branch power flow constraints, thermal power units constraints, hydropower unit constraint, wind and photovoltaic outputs constraints, and so on in the adjustment stage.

Combining the day-ahead operation and the additional adjustment a model is represented by (3). The model can achieve the minimum cost dispatch scheme x under the worst-case scenario considering the uncertainties of wind and photovoltaic outputs.

$$\begin{aligned} \min_{x} \quad & \left\{C_{\mathrm{ope}}(x)+\max_{u\in U}\ \min_{y\in\Omega(x,u)} C^{+}_{\mathrm{ope}}(u,y)\right\} \\ \text{s.t.} \quad & A_{\mathrm{ope}}(x)=0, \\ & B_{\mathrm{ope}}(x)\le 0 \\ & A^{+}_{\mathrm{ope}}(y)=0, \\ & B^{+}_{\mathrm{ope}}(y)\le 0 \end{aligned} \tag{3}$$

In (3), x is a type of "here-and-now" variable which represents the optimal day-ahead dispatch scheme under the worst-case scenario. In addition, it can hedge against any possible condition within the uncertain sets; y is a type of "wait-and-see" variable which represents the optimal adjustment scheme under the worst-case scenario. And it can vary with different operation conditions.

To clarify the model represented by (3), Section 2.2 presents the uncertain parameter u; Section 2.3 presents the objective function considering $C_{\mathrm{ope}}(\cdot)$ and $C^{+}_{\mathrm{ope}}(\cdot)$; Section 2.4 presents the day-ahead constraints $A_{\mathrm{ope}}(\cdot)$, $B_{\mathrm{ope}}(\cdot)$ and the adjustment constraints $A^{+}_{\mathrm{ope}}(\cdot)$, $B^{+}_{\mathrm{ope}}(\cdot)$.

2.2. Uncertain Parameter. The uncertain variable u is highly related to the outputs of the wind power and the photovoltaic power. Based on the uncertain set [28, 29], the outputs of the wind power and the photovoltaic power can be represented by the intervals shown by

$$\begin{aligned} P_{\mathrm{WTG},t} &\in \left[P^{\mathrm{pre}}_{\mathrm{WTG},t}-P^{\mathrm{flu}}_{\mathrm{WTG},t},\ P^{\mathrm{pre}}_{\mathrm{WTG},t}+P^{\mathrm{flu}}_{\mathrm{WTG},t}\right] \\ P_{\mathrm{PVG},t} &\in \left[P^{\mathrm{pre}}_{\mathrm{PVG},t}-P^{\mathrm{flu}}_{\mathrm{PVG},t},\ P^{\mathrm{pre}}_{\mathrm{PVG},t}+P^{\mathrm{flu}}_{\mathrm{PVG},t}\right] \end{aligned} \tag{4}$$

where $P^{\mathrm{pre}}_{\mathrm{WTG},t}$ is the predicted value of the wind power output at time t; $P^{\mathrm{pre}}_{\mathrm{PVG},t}$ is the predicted value of the photovoltaic power output at time t; $P^{\mathrm{flu}}_{\mathrm{WTG},t}$ and $P^{\mathrm{flu}}_{\mathrm{PVG},t}$ are the maximum fluctuation ranges of the wind power output and the photovoltaic power output, respectively.

Additionally, this paper also employs the adjustable robust parameters shown by

$$\begin{aligned} \sum_{t=1}^{T}\left|\frac{P_{\mathrm{WTG},t}-P^{\mathrm{pre}}_{\mathrm{WTG},t}}{P^{\mathrm{pre}}_{\mathrm{WTG},t}}\right| &\le \Gamma_{\mathrm{WTG}} \\ \sum_{t=1}^{T}\left|\frac{P_{\mathrm{PVG},t}-P^{\mathrm{pre}}_{\mathrm{PVG},t}}{P^{\mathrm{pre}}_{\mathrm{PVG},t}}\right| &\le \Gamma_{\mathrm{PVG}} \end{aligned} \tag{5}$$

where T is the simulation period; Γ_{WTG} and Γ_{PVG} are the adjustable robust parameter of the wind power output and the photovoltaic power output, respectively.

2.3. Objective Function. To achieve the optimal economical day-ahead dispatch scheme x, costs in different stages are considered. In the first stage the cost is mainly the generation cost of thermal power units C_{TMG}. The costs in the second stage mainly include the adjustment cost of thermal units $C^{\mathrm{delta}}_{\mathrm{TMG}}$, the adjustment cost of hydrounits $C^{\mathrm{delta}}_{\mathrm{HDG}}$, the wind power curtailment cost $C^{\mathrm{loss}}_{\mathrm{WTG}}$, and the photovoltaic power curtailment cost $C^{\mathrm{loss}}_{\mathrm{PVG}}$. The objective function is represented by

$$C_{\mathrm{ope}}=C_{\mathrm{TMG}}=\sum_{t=1}^{T}\left(a\cdot P^{2}_{\mathrm{TMG},t}+b\cdot P_{\mathrm{TMG},t}+c\right)$$

$$\begin{aligned} C^{+}_{\mathrm{ope}} &= C^{\mathrm{delta}}_{\mathrm{TMG}}+C^{\mathrm{delta}}_{\mathrm{HDG}}+C^{\mathrm{loss}}_{\mathrm{WTG}}+C^{\mathrm{loss}}_{\mathrm{PVG}}=\sum_{t=1}^{T}\Big[\lambda_{\mathrm{TMG}} \\ &\cdot\Delta P_{\mathrm{TMG},t}+\lambda_{\mathrm{HDG}}\cdot\Delta P_{\mathrm{HDG},t}+\lambda^{\mathrm{loss}}_{\mathrm{WTG}} \\ &\cdot\left(P_{\mathrm{WTG},t}-P^{\mathrm{get}}_{\mathrm{WTG},t}\right)+\lambda^{\mathrm{loss}}_{\mathrm{PVG}}\cdot\left(P_{\mathrm{PVG},t}-P^{\mathrm{get}}_{\mathrm{PVG},t}\right)\Big] \end{aligned} \tag{6}$$

where a, b, and c are the coefficient of the thermal power units; $P_{\mathrm{TMG,t}}$ is the outputs of the thermal power units at time t; λ_{TMG} and λ_{HDG} are the penalty prices for the adjustment power of thermal units and hydrounits; $\lambda^{\mathrm{loss}}_{\mathrm{WTG}}$

and $\lambda_{\mathrm{PVG}}^{\mathrm{loss}}$ are the penalty prices of wind power curtailment and photovoltaic power curtailment; $\Delta P_{\mathrm{TMG},t}$ and $\Delta P_{\mathrm{TMG},t}$ are the output adjustment of thermal power and hydropower at time t; $P_{\mathrm{WTG},t}^{\mathrm{get}}$ and $P_{\mathrm{PVG},t}^{\mathrm{get}}$ are the wind power and photovoltaic power which are injected into the power grid at time t.

2.4. Constraints

2.4.1. Day-Ahead Dispatch Constraints. Day-ahead dispatch constraints in the model represented by (3) contain the following:

(a) Thermal Power Constraints

$$S_{\mathrm{TMG},t} \cdot P_{\mathrm{TMG}}^{\min} \le P_{\mathrm{TMG},t} \le S_{\mathrm{TMG},t} \cdot P_{\mathrm{TMG}}^{\max} \tag{7}$$

$$-R_{\mathrm{TMG}}^{\mathrm{down}} \le P_{\mathrm{TMG},t+1} - P_{\mathrm{TMG},t} \le R_{\mathrm{TMG}}^{\mathrm{up}} \tag{8}$$

where $S_{\mathrm{TMG},t}$ is the 0-1 variable which denotes the unit commitment status of the thermal power at time t; $P_{\mathrm{TMG}}^{\max}$ and $P_{\mathrm{TMG}}^{\min}$ are the upper limit and the lower limit of the outputs of the thermal units; $R_{\mathrm{TMG}}^{\mathrm{up}}$ and $R_{\mathrm{TMG}}^{\mathrm{down}}$ are the upward and downward ramping capability of the thermal power units.

(*b) Hydropower Constraints*

$$P_{\mathrm{HDG}}^{\min} \le P_{\mathrm{HDG},t} \le P_{\mathrm{HDG}}^{\max} \tag{9}$$

$$U_{\mathrm{HDG},t} = \lambda_{\mathrm{HDG}}^{\mathrm{a}} \cdot P_{\mathrm{HDG},t} + \lambda_{\mathrm{HDG}}^{\mathrm{b}} \tag{10}$$

$$v_{\mathrm{flow}}^{\min} \le U_{\mathrm{HDG},t} \le v_{\mathrm{flow}}^{\max} \tag{11}$$

$$v_{\mathrm{dpm}}^{\min} \le U_{\mathrm{HDG},t} + U_{\mathrm{HDG},t}^{\mathrm{loss}} \le v_{\mathrm{dpm}}^{\max} \tag{12}$$

$$U_{t+1} = U_t + v_{\mathrm{in},t} - U_{\mathrm{HDG},t} - U_{\mathrm{HDG},t}^{\mathrm{loss}} \tag{13}$$

$$U^{\min} \le U_t \le U^{\max} \tag{14}$$

$$U_1 = U_{\mathrm{ini}} \tag{15}$$

$$U_T = U_{\mathrm{term}} \tag{16}$$

where $U_{\mathrm{HDG},t}$ is the water consumption of the hydrogenerators at time t; $P_{\mathrm{HDG},t}$ is the output of the hydrogenerators at time t; $\lambda_{\mathrm{HDG}}^{\mathrm{a}}$ and $\lambda_{\mathrm{HDG}}^{\mathrm{b}}$ are the converting coefficients of hydrogenerators; $v_{\mathrm{flow}}^{\max}$ and $v_{\mathrm{flow}}^{\min}$ are the upper and lower limit of water consumption in every subperiod; $U_{\mathrm{HDG},t}^{\mathrm{loss}}$ is the water curtailment of reservoir; U_t is the reservoir storage at time t; $v_{\mathrm{in},t}$ is the amount of water that flows into the reservoir at time t; $U^{\max}$ and $U^{\min}$ are the upper limit and the lower limit of the reservoir storage. U_{ini} and U_{term} are the initial value and final value of the reservoir storage.

(c) Power Balance Constraint

$$P_{\mathrm{TMG},t} + P_{\mathrm{HDG},t} + P_{\mathrm{WTG},t}^{\mathrm{pre}} + P_{\mathrm{PVG},t}^{\mathrm{pre}} = P_{\mathrm{LOAD,t}} \tag{17}$$

where $P_{\mathrm{LOAD},t}$ is the power demand of the load in the system at time t.

(d) Branch Flow Constraint

$$\left| \sum_{b=1}^{N_b} \kappa_{lb} \cdot \mathrm{P}_{b,t} \right| \le P_l^{\max} \tag{18}$$

where l is the identifier number of the transmission lines; b is the identifier number of the nodes; N_b is the total number of the nodes; κ_{lb} is the sensitivity factor of the l^{th} line to the b^{th} node; $P_{b,t}$ is the net active power which is injected into the b^{th} node at time t; $P_l^{\max}$ is the maximum transmission power of the l^{th} line.

2.4.2. Additional Adjustment Constraints. Additional adjustment constraints in the model represented by (3) contain the following:

(a) Thermal Power Units Regulation Constraints

$$\begin{aligned} \Delta S_{\mathrm{TMG},t} \cdot \Delta P_{\mathrm{TMG}}^{\min} &\le \left|\Delta P_{\mathrm{TMG},t}\right| \le \Delta S_{\mathrm{TMG},t} \cdot \Delta P_{\mathrm{TMG}}^{\max} \\ S_{\mathrm{TMG},t} \cdot P_{\mathrm{TMG}}^{\min} &\le P_{\mathrm{TMG},t} + \Delta P_{\mathrm{TMG},t} \le S_{\mathrm{TMG},t} \cdot P_{\mathrm{TMG}}^{\max} \\ -R_{\mathrm{TMG}}^{\mathrm{down}} &\le P_{\mathrm{TMG},t+1} + \Delta P_{\mathrm{TMG},t+1} - P_{\mathrm{TMG},t} \\ &\quad - \Delta P_{\mathrm{TMG},t} \le R_{\mathrm{TMG}}^{\mathrm{up}} \end{aligned} \tag{19}$$

where $\Delta S_{\mathrm{TMG},t}$ is the 0-1 variable which represents the adjustment status of the thermal power units at time t; $\Delta P_{\mathrm{TMG}}^{\max}$ and $\Delta P_{\mathrm{TMG}}^{\min}$ are the upper and lower adjustment limits of the thermal power units. Equation (19) guarantees that the adjusted outputs should still be constrained in the permissible range.

(b) Hydropower Units Regulation Constraints

$$\Delta \mathrm{S}_{\mathrm{HDG},t} \cdot \Delta P_{\mathrm{HDG}}^{\min} \le \left|\Delta P_{\mathrm{HDG},t}\right| \le \Delta \mathrm{S}_{\mathrm{HDG},t} \cdot \Delta P_{\mathrm{HDG}}^{\max} \tag{20}$$

$$\begin{aligned} P_{\mathrm{HDG}}^{\min} &\le P_{\mathrm{HDG},t} + \Delta P_{\mathrm{HDG},t} \le P_{\mathrm{HDG}}^{\max} \\ U_{\mathrm{HDG,rt},t} &= \lambda_{\mathrm{HDG}}^{\mathrm{a}} \cdot \left(P_{\mathrm{HDG},t} + \Delta P_{\mathrm{HDG},t}\right) \\ &\quad + \lambda_{\mathrm{HDG}}^{\mathrm{b}} \\ v_{\mathrm{flow}}^{\min} &\le U_{\mathrm{HDG,rt},t} \le v_{\mathrm{flow}}^{\max} \\ v_{\mathrm{dpm}}^{\min} &\le U_{\mathrm{HDG,rt},t} + U_{\mathrm{HDG,rt},t}^{\mathrm{loss}} \le v_{\mathrm{dpm}}^{\max} \\ U_{\mathrm{rt},t+1} &= U_{\mathrm{rt},t} + v_{\mathrm{in},t} - U_{\mathrm{HDG,rt},t} - U_{\mathrm{HDG,rt},t}^{\mathrm{loss}} \\ U^{\min} &\le U_{\mathrm{rt},t} \le U^{\max} \end{aligned} \tag{21}$$

where $\Delta \mathrm{S}_{\mathrm{HDG},t}$ is the binary variable which represents the adjustment status of hydrogenerators at time t; $\Delta P_{\mathrm{HDG}}^{\max}$ and $\Delta P_{\mathrm{HDG}}^{\min}$ are the upper and lower limit of the hydrogenerator adjustment power; $U_{\mathrm{HDG,rt},t}$ is the water consumption after the adjustment at time t; $U_{\mathrm{HDG,rt},t}^{\mathrm{loss}}$ is the water curtailment of reservoir after the adjustment at time t; $U_{\mathrm{rt},t}$ is the reservoir storage after the adjustment at time t. The constraints (21) guarantee that the hydropower should still be constrained in the permissible range after the adjustment.

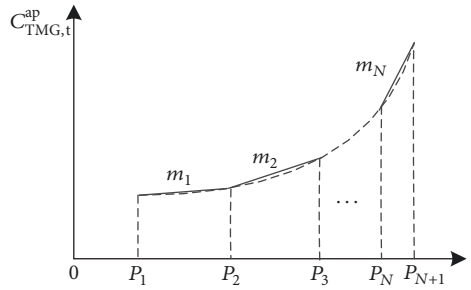

Figure 1: Piecewise linearizing of generation cost curve of thermal units.

(c) Power Balance Constraint

$$\left(P_{\mathrm{TMG},t} + \Delta P_{\mathrm{TMG},t}\right) + \left(P_{\mathrm{HDG},t} + \Delta P_{\mathrm{HDG},t}\right) + P^{\mathrm{get}}_{\mathrm{WTG},t} + P^{\mathrm{get}}_{\mathrm{PVG},t} = P_{\mathrm{LOAD},t} \tag{22}$$

Equation (22) indicates that the outputs of multiple powers after adjustment should equal to the power consumption of the load in the power system at time t.

(d) Branch Flow Constraint

$$\left|\sum_{b=1}^{N_b} \kappa_{lb} \cdot \mathrm{P}_{\mathrm{rt},b,t}\right| \le P_l^{\max} \tag{23}$$

where $\mathrm{P}_{\mathrm{rt},b,t}$ is the net active power injected into the b^{th} node after adjustment at time t.

(e) Wind Power Constraint

$$0 \le P^{\mathrm{get}}_{\mathrm{WTG},t} \le P_{\mathrm{WTG,t}} \tag{24}$$

where $P_{\mathrm{WTG},t}$ is the actual output of wind turbine generators at time t, which is an uncertainty variable.

(f) Photovoltaic Power Constraint

$$0 \le P^{\mathrm{get}}_{\mathrm{PVG},t} \le P_{\mathrm{PVG,t}} \tag{25}$$

where $P_{\mathrm{PVG},t}$ is the actual output of photovoltaic generators at time t, which is an uncertainty variable.

3. Linearization of Thermal Power Generation Cost

The day-ahead economical dispatch is a mixed integer quadratic programming (MIQP) problem. Using robust optimization directly may be time consuming to achieve the optimal solution. Therefore, this paper employs piecewise linearization approximation [30] to convert the MIQP problem into a mixed integer linear programming (MILP) problem.

In our model, the nonlinear factor (the first equation in (6)) exists only in thermal power. Figure 1 shows the relationship of the power system operating cost and thermal power output according to the first equation in (6). To linearize the relationship, piecewise-linear approximation is employed. Firstly, we segment the curve into a number of N segments. And then in each segment, by employing the continuous variable $P_{j,t}$ and the state variable $S_{j,t}$, linear approximation can been done. As a result, the linearized cost of the thermal units is presented by

$$C^{\mathrm{ap}}_{\mathrm{TMG,t}} = \sum_{j=1}^{N} \left(m_j P_{j,t} + n_j S_{j,t}\right) \tag{26}$$

$$\begin{aligned} m_j &= \frac{C^{\mathrm{ap}}_{\mathrm{TMG},t+1} - C^{\mathrm{ap}}_{\mathrm{TMG},t}}{P_{j,t+1} - P_{j,t}} \\ n_j &= C^{\mathrm{ap}}_{\mathrm{TMG},t} - P_{j,t} \cdot m_j \\ P_j \cdot S_{j,t} &\le P_{j,t} \le P_{j+1} S_{j,t} \\ S_{\mathrm{TMG},t} &= \sum_{j=1}^{N} n_{j,t} \le 1 \end{aligned} \tag{27}$$

where $C^{\mathrm{ap}}_{\mathrm{TMG},t}$ is the linearized cost function of the thermal units; m_j is the slope of j^{th} segmentation; n_j is the intercept of the j^{th} segmentation; $P_{j,t}$ is the output of the j^{th} segmentation; $S_{j,t}$ is the status of the j^{th} segmentation at time t; P_j is the j^{th} segmentation point.

Based on the linearization, the original two-stage model can be represented using the matrix shown by

$$\begin{aligned} \text{OP:} \\ \min_{\boldsymbol{x}} \quad & \left\{\boldsymbol{d}^{\mathrm{T}}\boldsymbol{x} + \max_{\boldsymbol{u}\in U} \min_{\boldsymbol{y}} \left(\boldsymbol{e}^{\mathrm{T}}\boldsymbol{y} + \boldsymbol{f}^{\mathrm{T}}\boldsymbol{u}\right)\right\} \\ \text{s.t.} \quad & \boldsymbol{D}\boldsymbol{x} \le \boldsymbol{g}, \\ & \boldsymbol{F}\boldsymbol{x} + \boldsymbol{G}\boldsymbol{y} \le \boldsymbol{h}, \\ & \boldsymbol{I}_{\mathrm{u}}\boldsymbol{y} \le \boldsymbol{u} \end{aligned} \tag{28}$$

where $\boldsymbol{d}$, $\boldsymbol{e}$, and $\boldsymbol{f}$ are the coefficient matrices in the objective function; $\boldsymbol{D}$, $\boldsymbol{F}$, $\boldsymbol{G}$, and $\boldsymbol{I}_{\mathrm{u}}$ are the coefficient matrices in the constraints; $\boldsymbol{g}$ and $\boldsymbol{h}$ are the column vectors; $\boldsymbol{x}$ is the vector of all the first-stage decisions; $\boldsymbol{y}$ is the vector of all the second stage decisions; $\boldsymbol{u}$ is the vector of all the uncertainty variables.

4. Solution for the Model

4.1. Model Decomposition. In our model, the worst scenario and its corresponding additional adjustment scheme in the second stage are optimized based on the day-ahead dispatch scheme in the first-stage optimization. Moreover, the optimization in the second stage also impacts the optimized results of the first stage. The interactions between the two stages result in the employment of C&CG algorithm [18] to decompose the original model into the MP (Master Problem) and SP1 (Subproblem). Additionally, in MP an auxiliary variable η is adopted to substitute for the objective of SP1.

$$\begin{aligned}
&\text{MP:}\\
&\min_{\boldsymbol{x}} \quad \boldsymbol{d}^{\mathrm{T}}\boldsymbol{x} + \eta\\
&\text{s.t.} \quad \eta \geq \boldsymbol{e}^{\mathrm{T}}\boldsymbol{y} + \boldsymbol{f}^{\mathrm{T}}\boldsymbol{u}\\
&\qquad \boldsymbol{D}\boldsymbol{x} \leq \boldsymbol{g},\\
&\qquad \boldsymbol{F}\boldsymbol{x} + \boldsymbol{G}\boldsymbol{y} \leq \boldsymbol{h},\\
&\qquad \boldsymbol{I}_{\mathrm{u}}\boldsymbol{y} \leq \boldsymbol{u}
\end{aligned} \tag{29}$$

$$\begin{aligned}
&\text{SP1:}\\
&\max_{\boldsymbol{u}\in U}\min_{\boldsymbol{y}} \quad \left(\boldsymbol{e}^{\mathrm{T}}\boldsymbol{y} + \boldsymbol{f}^{\mathrm{T}}\boldsymbol{u}\right)\\
&\text{s.t.} \quad \boldsymbol{F}\boldsymbol{x} + \boldsymbol{G}\boldsymbol{y} \leq \boldsymbol{h},\\
&\qquad \boldsymbol{I}_{\mathrm{u}}\boldsymbol{y} \leq \boldsymbol{u}
\end{aligned} \tag{30}$$

4.2. The Equivalent Maximization Problem of SP1. This paper employs strong duality theory to convert the SP1 into an equivalent maximization problem. Big-M approach is also adopted to handle the nonlinear terms in the dual problem. The converted SP2 is represented in

$$\begin{aligned}
&\text{SP2:}\\
&\max_{\boldsymbol{u},\boldsymbol{\alpha},\boldsymbol{\beta}} \quad \boldsymbol{h}^{\mathrm{T}}\boldsymbol{\alpha} - \boldsymbol{x}^{\mathrm{T}}\boldsymbol{F}^{\mathrm{T}}\boldsymbol{\alpha} + \boldsymbol{u}^{+}\boldsymbol{\theta}^{+} + \boldsymbol{u}^{-}\boldsymbol{\theta}^{-}\\
&\qquad\qquad + \boldsymbol{u}^{0}\left(1 - \boldsymbol{\theta}^{+} - \boldsymbol{\theta}^{-}\right)\\
&\text{s.t.} \quad \boldsymbol{G}^{\mathrm{T}}\boldsymbol{\alpha} + \boldsymbol{I}_{\mathrm{u}}{}^{\mathrm{T}}\boldsymbol{\beta} = \boldsymbol{e},\\
&\qquad \boldsymbol{\alpha} \leq 0,\\
&\qquad \boldsymbol{\beta} \leq 0,\\
&\qquad \boldsymbol{\theta} = \boldsymbol{f} + \boldsymbol{\beta}\\
&\qquad -M\left(1 - \mu_t^{+}\right) + \theta_t \leq \theta_t^{+} \leq M\left(1 - \mu_t^{+}\right) + \theta_t\\
&\qquad -M\left(1 - \mu_t^{-}\right) + \theta_t \leq \theta_t^{-} \leq M\left(1 - \mu_t^{-}\right) + \theta_t\\
&\qquad -M\mu_t^{+} \leq \theta_t^{+} \leq M\mu_t^{+},\\
&\qquad -M\mu_t^{-} \leq \theta_t^{-} \leq M\mu_t^{-}\\
&\qquad \mu_t^{+} + \mu_t^{-} \leq 1,\\
&\qquad \sum_t \left(\mu_t^{+} + \mu_t^{-}\right) \leq \Gamma
\end{aligned} \tag{31}$$

where $\boldsymbol{\alpha}$, $\boldsymbol{\beta}$, $\boldsymbol{\gamma}$ are the dual variables; $\boldsymbol{u}^{+}$,$\boldsymbol{u}^{-}$ are the upper and lower limit of uncertainty variable; $\boldsymbol{u}^{0}$ is the predictive value of uncertainty variable; $\boldsymbol{\theta}^{+}$, $\boldsymbol{\theta}^{-}$ are the positive and negative values of $\boldsymbol{\theta}$; μ_t^{+}, μ_t^{-} are the binary variables introduced by the Big-M approach; the adjustable robust parameter Γ includes Γ_{WTG} and Γ_{PVG}.

4.3. Iterations between MP and SP2. Our model is finally converted into the MP and the SP2. The optimizations of OP (28) can be ultimately achieved based on the iterations using the following steps.

Step 1 (initialization). Initialize the worst-case scenario $\boldsymbol{u}_1$. Set the upper bound of the problem $U = +\infty$ and the lower bound of the problem L=-∞. Set the number of iterations k=1 and the convergence gap $\lambda > 0$.

Step 2 (master problem computation). According to the worst scenario $\boldsymbol{u}_l$ (l=1, 2, . . ., k), solve the MP and achieve the optimal solution ($\boldsymbol{x}_k$, η,$\boldsymbol{y}_1$,$\boldsymbol{y}_2$, . . .,$\boldsymbol{y}_k$), and then set $L = \eta$.

Step 3 (subproblem computation). After given the first-stage solutions $x = x_k$, the solution ($\boldsymbol{u}_k^{o}$, $\boldsymbol{y}_k^{o}$) of the SP2 can be obtained. Set the worst-case scenario $\boldsymbol{u}_{k+1} = \boldsymbol{u}_k^{o}$, $U = \boldsymbol{e}^{\mathrm{T}}\boldsymbol{y}_k^{o} + \boldsymbol{f}^{\mathrm{T}}\boldsymbol{u}_k^{o}$.

Step 4 (convergence check). If U-$L \leq \lambda$, return the solution x=x_k. Otherwise add the new variable $\boldsymbol{y}_{k+1}$ and the following constraints (32) which are associated with the new worst-case scenario, then update $k = k$+1 and go to Step 2 iteratively.

$$\begin{aligned}
&\text{Add:} \quad \eta \geq \boldsymbol{e}^{\mathrm{T}}\boldsymbol{y}_{k+1} + \boldsymbol{f}^{\mathrm{T}}\boldsymbol{u}_{k+1}\\
&\qquad \boldsymbol{F}\boldsymbol{x} + \boldsymbol{G}\boldsymbol{y}_{k+1} \leq \boldsymbol{h},\\
&\qquad \boldsymbol{I}_{\mathrm{u}}\boldsymbol{y}_{k+1} \leq \boldsymbol{u}_{k+1}
\end{aligned} \tag{32}$$

5. Experimental Result

To evaluate the effectiveness of the presented two-stage robust optimal model in enabling the economical day-ahead dispatch considering the uncertainties, this paper implements the model using MATLAB. The solution of the model is by employing CPLEX. A modified IEEE-30 bus system is employed as the power system model. The load fluctuations are shown in Figure 9. The parameters of the thermal power units are shown in Table 5. This paper only considers one case that the wind power, photovoltaic power and hydropower are connected at the same node (No. 30) in the IEEE-30 bus system. The capacity of the hydropower is 18MW while the other parameters are listed in Table 6. The capacity of the wind power is 10MW and the capacity of the photovoltaic power is 10MW. Additionally, according to the research [29], the fluctuations and the uncertain intervals of the wind power and photovoltaic power are shown in Figures 10 and 11. The penalty price of the wind power and photovoltaic power curtailed is 10$/MWh.

5.1. Experimental Result of the Two-Stage Robust Optimization. The values of Γ_{WTG} and Γ_{PVG} are set to 10 and 6. During the solution of the two-stage robust model, the C&CC approach converges after 6 iterations, which is shown in Figure 2. The final optimized thermal power output and the hydropower output are shown in Figure 3. The worst scenarios of the wind power and the photovoltaic power are shown in Figure 4.

Figure 3 indicates that, compared to the traditional deterministic optimization, the output of the hydropower optimized by the robust optimization is lower in the period of 8h-24h. Contrarily, the output of the thermal power becomes higher. The reason is that the robust optimization considers the worst scenario of both wind power and photovoltaic

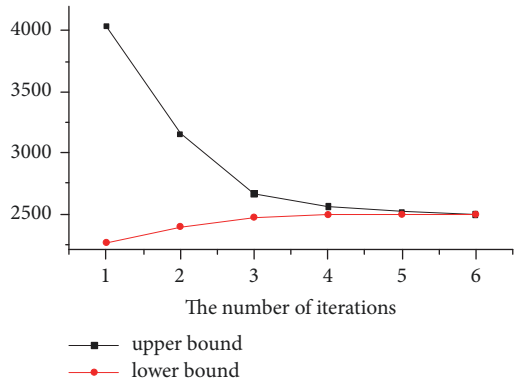

Figure 2: Convergence of C&CG approach.

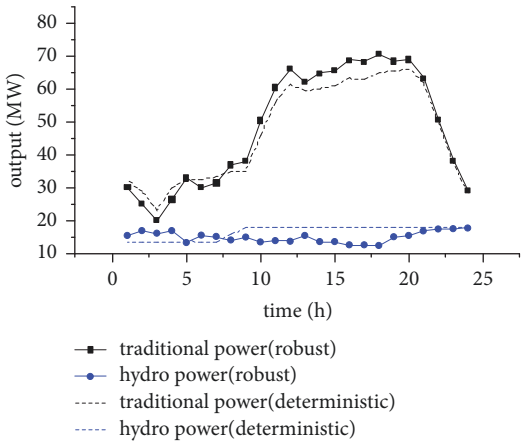

Figure 3: The output power of thermal units and hydrounits.

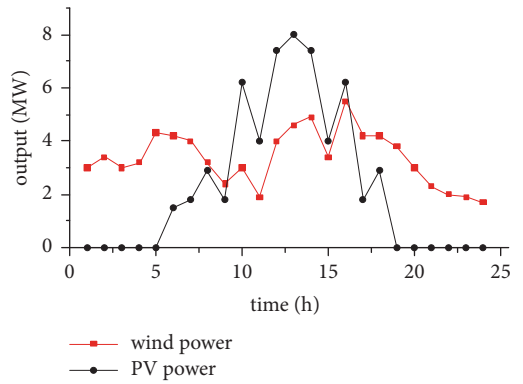

Figure 4: The worst-case scenario of WTG and PVG.

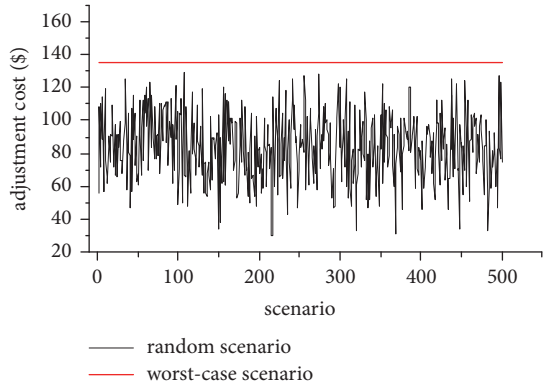

Figure 5: Robustness analysis.

power. In the worst scenario, the output of both wind and photovoltaic power may be lower than the predicted values. As a result, thermal power and hydropower need to output more to compensate the imbalance. Additionally, more adjustment space of hydropower has been reserved at 8h-24h to handle the uncertainties of the renewable energies. As the adjustment ability of the hydropower is flexible and also the cost of the hydropower is lower, this point significantly reduces the adjustment demand of the thermal power leading to the economical dispatch scheme.

Under the robust optimized dispatch scheme, the day-ahead operation cost is 2359.9 USD while the adjustment cost under the worst-case scenario is 134.8 USD. To evaluate the robustness based on the adjustable robust parameter constraints, this paper also employs Monte Carlo approach to generate a number of 500 random scenarios. The adjustment cost of each scenario is calculated based on the robust optimized day-ahead dispatch scheme. Figure 5 shows that the presented approach can identify the worst-case scenario and it can calculate the adjustment cost under the worst-case.

5.2. Analysis of the Economy of the Dispatch Scheme. The economy of the optimized dispatch scheme is evaluated by the number of 500 scenarios generated by Monte Carlo approach. The adjustable robust parameter in the static robust planning is as the same as the two-stage robust planning. The comparisons are listed in Table 1.

Three points can be clearly seen in Table 1. (a) Although the two-stage robust optimized day-ahead operating cost is higher than that of the deterministic optimization, the total cost has been greatly reduced compare to that of the deterministic optimization (no charge for wind power and PV power curtailment). (b) Although the adjustable robust parameter has been introduced, the day-ahead operation cost of the static robust planning remains high. In addition, the wind power curtailment and PV power curtailment still occur. Moreover, the total cost for the static robust model is higher than the two-stage robust model. (c) Based on the two-stage robust optimization, neither wind power curtailment nor PV power curtailment occurs, which greatly improves the accommodation capability of the renewable energies.

As mentioned in the introduction section, the hydropower has strong adjusting ability. And it should be also pointed out that robust model considers the worst-case scenario, in which the output of both wind and photovoltaic power may be lower than the predicted values. Thus, in the robust scheme, hydrounits retain more capacity of upregulation than that in the deterministic scheme to ensure the economic benefits. As a result, though the adjustment cost of hydropower increases, the total adjustment cost is significantly decreased.

Table 1: Comparison for operation costs.

Category		Two-stage robust planning		Static robust planning		Deterministic planning	
		Avg.	Max	Avg.	Max	Avg.	Max
Day-ahead operation cost /$		2359.9		2374.2		2264.1	
Adjustment cost /$	Thermal units	2.7	30.8	85.0	251.5	375.9	1153.7
	Hydro units	123.2	169.4	153.9	221.8	51.1	145.3
	Wind power curtailment	0	0	73.0	500.9	314.9	1053.1
	PV power curtailment	0	0	53.1	473.2	225.2	813.9
Total cost /$		2485.8	2541.4	2739.2	3348.3	3231.2	4098.5

Table 2: The effect of hydropower.

Category	*Case 1*		*Case 2*		*Case 3*		*Case 4*	
	Avg.	Max	Avg.	Max	Avg.	Max	Avg.	Max
Adjustment cost of thermal units /$	404.1	1109.5	21.2	107.9	2.7	30.8	0.5	7.2
Adjustment cost of hydro units /$	—	—	110.3	143.35	123.2	169.4	124.3	174.0
Wind power curtailment cost /$	154.2	1089.0	0	0	0	0	0	0
PV power curtailment cost /$	193.3	763.0	4.9	37.3	0	0	0	0
Total cost /$	751.6	1852.0	136.34	245.4	125.9	181.5	124.8	176.7

In addition, the two-stage robust model formulates a better base generation for thermal units and hydrounits than that of the static robust model based on the iterations between the main problem and the subproblem. Consequently, wind power curtailment cost and PV power curtailment cost are reduced to 0. The renewable energy resources accommodation capability of the power system is greatly enhanced.

5.3. The Importance Analysis of the Hydropower. To reveal the importance of the hydropower in the dispatch scheme, extra dispatch scheme optimizations with different hydropower penetrations have been carried out and evaluated. Four different cases are studied as listed below.

Case 1. Not considering the hydropower.

Case 2. The capacity of the hydropower is 9MW.

Case 3. The capacity of the hydropower is 18MW.

Case 4. The capacity of the hydropower is 30MW.

The results are shown in Figures 6 and 7.

It can be observed that, along with the hydropower penetration increases, the output of the thermal power decreases. As a result, the day-ahead operation cost can be reduced. In addition, the cost of the dispatch scheme also has been significantly impacted as shown in Table 2.

Table 2 indicates that in *Case 1*, thermal power has to deal with the uncertainties of the renewable energies. This point leads to higher adjustment cost. Even in some scenarios, adjustment demand exceeds the adjustment capacity which causes wind power curtailment and PV power curtailment. Therefore, the total cost further increases. In *Case 2*, hydropower participates in managing power imbalance. It shares the adjustment pressure with thermal power. Therefore, the total adjustment cost is greatly reduced. However,

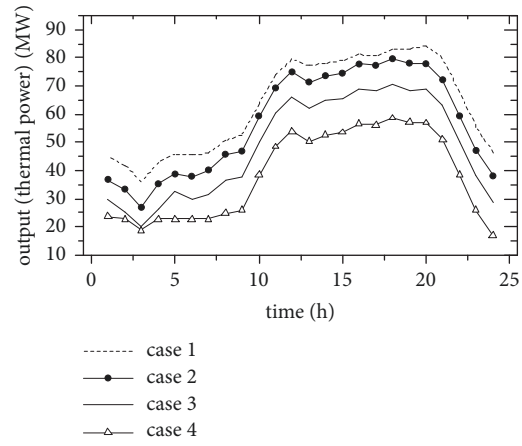

Figure 6: The output power of thermal units in different cases.

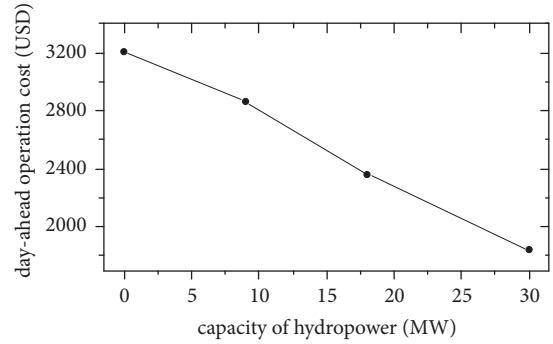

Figure 7: Day-ahead operation cost in different cases.

PV power curtailment still occurs in this case. In *Case 3* and *Case 4*, neither wind power curtailment nor PV power curtailment occurs. Compared to *Case 3*, the decline of the adjustment cost in *Case 4* is less. It indicates that when the

Table 3: Optimization results and economic efficiency with different adjustable robust parameter Γ.

Category	Γ_{WTG}=0, Γ_{PVG}=0		Γ_{WTG}=10, Γ_{PVG}=6		Γ_{WTG}=24, Γ_{PVG}=24	
	Avg.	Max	Avg.	Max	Avg.	Max
Day-ahead operation cost /$	2264.1		2359.9		2430.0	
Adjustment cost /$	969.6	1831.8	125.9	181.5	123.4	169.4
Total cost /$	3233.7	4095.9	2485.8	2541.4	2553.4	2599.4

Table 4: Adjustment cost under different adjustable prediction error.

Category	α=0		α=0.25		α=0.5		α=0.75		α=1	
	Avg.	Max	Avg.	Max	Avg.	Max	Avg.	Max	Avg.	Max
Adjustment cost of thermal units /$	0	0	0	0	0.6	10.6	2.6	28.1	2.7	30.8
Adjustment cost of hydro units /$	0	0	31.3	42.3	61.2	83.6	91.2	122.4	123.2	169.4
Wind power curtailment cost /$	0	0	0	0	0	0	0	0	0	0
PV power curtailment cost /$	0	0	0	0	0	0	0	0	0	0
total adjustment cost /$	0	0	31.3	42.3	61.9	83.6	93.8	148.0	125.9	181.5

hydropower capacity reaches to 18MW, the power system has a strong ability to cope with the risks due to the uncertainties of the renewable energy sources. Additionally, the experiment also suggests that, to handle the uncertainties of the wind power and PV power, hydropower significantly outperforms the thermal power.

5.4. The Impact of Adjustable Robust Parameter. The previous experiments are based on the values of the adjustable robust parameter Γ_{WTG}=10 and Γ_{PVG}=6. In this section another two groups of adjustable robust parameter Γ_{WTG}=0, Γ_{PVG}=0 and Γ_{WTG}=24, Γ_{PVG}=24 are also employed to study the impact of the optimal dispatch scheme under different values of Γ. Table 3 shows the comparisons.

Table 3 indicates that when the values of the uncertain parameters are 0, the result of the robust optimization is close to that of the deterministic optimization. However, when the values of the uncertain parameters are 24, the day-ahead operation cost and total cost become larger than those of Γ_{WTG}=10, Γ_{PVG}=6. This point shows if the values of the adjustable robust parameter are conservative, the performance of the optimization also becomes conservative.

5.5. The Impact of Prediction Error. In order to reveal the influence of the different prediction errors of the renewable energy sources in the two-stage robust model, the deviation indicator α of the fluctuation range is introduced. To simplify the problem, it assumes that the wind power and PV power have the same deviation indicator. The formula of the deviation is shown as (33):

$$\begin{aligned} \overset{\circ}{P}{}^{\text{flu}}_{\text{WTG},t} &= \alpha \cdot \overline{P}{}^{\text{flu}}_{\text{WTG},t} \\ \overset{\circ}{P}{}^{\text{flu}}_{\text{PVG},t} &= \alpha \cdot \overline{P}{}^{\text{flu}}_{\text{PVG},t} \end{aligned} \tag{33}$$

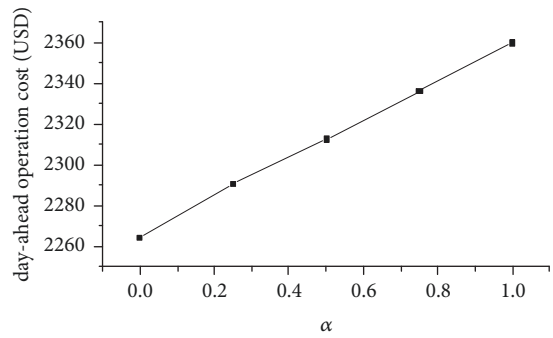

Figure 8: Comparison for the planning results under different prediction error.

where $\overline{P}{}^{\text{flu}}_{\text{WTG},t}$ and $\overline{P}{}^{\text{flu}}_{\text{PVG},t}$ are the fluctuation range of the wind power and PV power illustrated in the Figures 10 and 11.

In this section, five deviation indicators (0, 0.25, 0.5, 0.75, and 1) are employed to the presented model. The day-ahead operation cost under the different prediction error is shown in Figure 8. In addition, the adjustment cost is also greatly influenced as shown in Table 4.

As can be seen from Figure 8, the day-ahead operation cost increases with the increasing deviation indicator value. This is because that the worse scenarios are considered in the two-stage robust model. Additionally, the increasing adjustment cost also suggests that more generation adjustments are needed.

6. Conclusion

This paper presents a two-stage robust model in enabling economical day-ahead dispatch considering wind power, photovoltaic power, hydropower, and thermal power. Based on the model decomposition and linearization, the original

Table 5: The parameters of thermal generator.

Category	Node	P_{TMG}^{max}(MWh)	P_{TMG}^{min}(MWh)	R_{TMG}^{up}(MW/h)	R_{TMG}^{down}(MW/h)	a	b	c	λ_{TMG}($/Mwh)
1	1	40	10	15	10	0.02	2	0	8.152
2	2	40	10	20	15	0.0175	1.75	0	12.170
3	22	25	5	10	10	0.0625	1	0	7.771
4	27	22.5	5	10	8	0.00834	2.25	0	6.899
5	23	15	5	8	5	0.025	2	0	5.024
6	13	20	5	8	5	0.025	2	0	6.020

Table 6: The parameters of hydrogenerator.

λ_{HDG}^{a}(m^3/(Mwh))	λ_{HDG}^{b}(m^3/(Mwh))	v_{flow}^{max}(10^4m^3/h)	v_{flow}^{min}(10^4m^3/h)	v_{dpm}^{max}(10^4m^3/h)	v_{dpm}^{min}(10^4m^3/h)
2500	0	4.86	0	7.00	3.25
$v_{in,t}$(10^4m^3/h)	U^{max}(10^8m^3)	U^{min}(10^8m^3)	U_{ini}(10^8m^3)	U_{term}(10^8m^3)	λ_{HDG}($/Mwh)
4.10	1.3586	1.1623	1.3366	1.3366	3.5

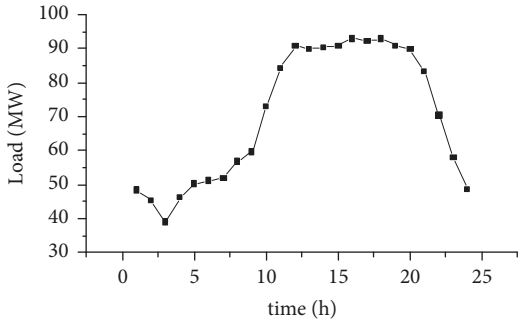

Figure 9: Load demand.

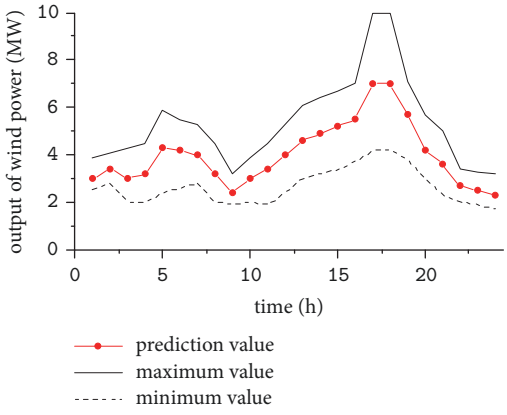

Figure 10: Wind power fluctuation interval.

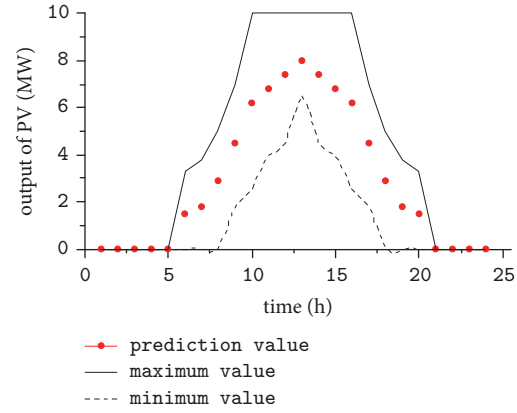

Figure 11: PV fluctuation interval.

model can be converted into MP and SP, which are finally handled by C&CG approach. Based on the experimental results, the contributions of the presented model are as follows:

(1) The two-stage robust model is able to achieve the optimal day-ahead dispatch scheme under the worst wind and photovoltaic output scenarios. The scheme is proved to be economy and has great potential to improve the capability of the power system to accommodate wind and photovoltaic power.

(2) Hydropower can effectively handle the uncertainties caused by wind power and photovoltaic power. In our model by considering the adjusting ability of the hydropower, the adjustment demand of the thermal unit can be significantly reduced. Additionally, the wind power curtailment and PV power curtailment can also be potentially avoided.

(3) The adjustable robust parameter enables the performance adjustment of the optimized dispatch scheme by tuning their values. As a result, the compromise between economy and robust could be achieved under different dispatching requirements.

Taking more factors (demand side management, battery storage system, electric vehicle [31], and so on) into account in wind-solar-hydropower system is our follow-up work in the future.

Appendix

See Figures 9, 10, and 11 and Tables 5 and 6.

Data Availability

The IEEE bus model used to support the findings of this study has been deposited in the Department of Electrical Engineering at the University of Washington. The details of the modifications of the models and the customized parameters are stated in the paper. IEEE bus model site is available at http://www.ee.washington.edu/research/pstca/.

Conflicts of Interest

The authors declare that there are no conflicts of interest regarding the publication of this article.

References

[1] Y. Bai, Y. Wang, Q. Xia, X. Sun, M. Yang, and J. Zhang, "A full-scenario SCED with coordinative optimization of hydro-thermal-wind power," *Proceedings of the Chinese Society of Electrical Engineering*, vol. 33, no. 13, pp. 1–9, 2013.

[2] L. Ye, X. Qu, Y. Yao et al., "Analysis on intraday operation characteristics of hybrid wind-solar-hydro power generation system," *Automation of Electric Power System*, vol. 42, no. 04, pp. 158–164, 2018.

[3] F. Arpino, M. Dell'Isola, D. Maugeri, N. Massarotti, and A. Mauro, "A new model for the analysis of operating conditions of micro-cogenerative SOFC units," *International Journal of Hydrogen Energy*, vol. 38, no. 1, pp. 336–344, 2013.

[4] F. Calise, R. D. Figaj, N. Massarotti, A. Mauro, and L. Vanoli, "Polygeneration system based on PEMFC, CPVT and electrolyzer: Dynamic simulation and energetic and economic analysis," *Applied Energy*, vol. 192, pp. 530–542, 2017.

[5] L. Chen, J. Chen, Z. Li et al., "Scheduling strategy of hybrid wind-photovoltaic-hydro power generation system," *Electric Power Construction*, vol. 34, no. 12, pp. 1–6, 2013.

[6] X. Yang, Q. Chen, M. Wang, and L. Zhang, "Cooperating control for wind farm and hydro power plant based on the fruit fly optimization," *Proceedings of the Chinese Society of Electrical Engineering*, vol. 37, no. 18, pp. 5286–5293, 2017.

[7] X. Yang, W. Wang, B. Xue et al., "On short-term united optimal operation of wind power, thermal power and water power," *Journal of Hydroelectric Engineering*, vol. 37, no. 18, pp. 5286–5293, 2017.

[8] J. A. Momoh and S. S. Reddy, "Review of optimization techniques for Renewable Energy Resources," in *Proceedings of the 2014 IEEE Symposium on Power Electronics and Machines for Wind and Water Applications, PEMWA 2014*, Milwaukee, WI, USA, July 2014.

[9] W. Gan, X. Ai, J. Fang, Y. Ta, and J. Wen, "Coordinated optimal operation of the wind, coal, hydro, gas units with energy storage," *Transactions of China Electrotechnical Society*, vol. 32, pp. 11–20, 2017.

[10] H. Liu, P. Daoxin, H. Xin et al., "Joint scheduling optimization model of multi-type generator with uncertainty," *Water Resources and Power*, vol. 34, no. 02, pp. 153–158, 2016.

[11] L. Li, W. Wu, and D. Shen, "Modeling and research of wind-pv-water hybrid power generation system," *East China Electric Power*, vol. 40, no. 07, pp. 1157–1160, 2012.

[12] X. Liu and W. Xu, "Economic load dispatch constrained by wind power availability: A here-and-now approach," *IEEE Transactions on Sustainable Energy*, vol. 1, no. 1, pp. 2–9, 2010.

[13] W. Dong, Q. Wang, and L. Yang, "A coordinated dispatching model for a distribution utility and virtual power plants with wind/photovoltaic/hydro generators," *Automation of Electric Power Systems*, vol. 39, no. 9, pp. 75–207, 2015.

[14] Y. Zou and L. Yang, "Synergetic dispatch models of a wind/PV/hydro virtual power plant based on representative scenario set," *Power System Technology*, vol. 39, no. 7, pp. 1855–1859, 2015.

[15] Y. Liu, C. Jiang, J. Shen, and J. Hu, "Coordination of Hydro Units with Wind Power Generation Using Interval Optimization," *IEEE Transactions on Sustainable Energy*, vol. 6, no. 2, pp. 443–453, 2015.

[16] C. Peng, P. Xie, J. Zhan, and H. Sun, "Robust economic dispatch of microgrid using improved bacterial foraging algorithm," *Power System Technology*, vol. 38, no. 9, pp. 2392–2398, 2014.

[17] Y. Yang, W. Pei, W. Deng, H. Xiao, and Z. Qi, "Optimal operation of grid-connected microgrid based on Benders decomposition," *Electric Power Automation Equipment*, vol. 34, no. 10, pp. 21–27, 2014.

[18] Y. Liu, L. Guo, and C. Wang, "Economic dispatch of microgrid based on two stage robust optimization," *Proceedings of the CSEE*, vol. 38, no. 14, pp. 4013–4022, 2018.

[19] S. Wang, Y. Niu, L. Fang et al., "Dual stage scheduling strategy for microgrid community considering uncertainty of renewable energy," *Power System Protection and Control*, vol. 46, no. 17, pp. 89–98, 2018.

[20] S. Surender Reddy, P. R. Bijwe, and A. R. Abhyankar, "Real-time economic dispatch considering renewable power generation variability and uncertainty over scheduling period," *IEEE Systems Journal*, vol. 99, pp. 1–12, 2015.

[21] S. Surender Reddy and P. R. Bijwe, "Day-ahead and real time optimal power flow considering renewable energy resources," *International Journal of Electrical Power & Energy Systems*, vol. 82, pp. 400–408, 2016.

[22] C. Ma, C. Dong, Z. Lü et al., "Short-term trading and optimal operation strategy for commercial virtual power plant considering uncertainties," *Power System Technology*, vol. 40, no. 5, pp. 1543–1549, 2016.

[23] S. S. Reddy, A. R. Abhyankar, and P. R. Bijwe, "Market clearing for a wind-thermal power system incorporating wind generation and load forecast uncertainties," in *Proceedings of the 2012 IEEE Power and Energy Society General Meeting, PES 2012*, USA, July 2012.

[24] Y. Wang and J. Zhao, "Optimal spinning reserve of power system with wind power penetrated under power market environment," *Power System and Clean Energy*, vol. 33, no. 7, pp. 123–128, 2017.

[25] S. S. Reddy, "Optimal scheduling of wind-thermal power system using clustered adaptive teaching learning based optimization," *Electrical Engineering*, vol. 99, no. 2, pp. 535–550, 2017.

[26] S. S. Reddy, P. R. Bijwe, and A. R. Abhyankar, "Optimum day-ahead clearing of energy and reserve markets with wind power generation using anticipated real-time adjustment costs," *International Journal of Electrical Power & Energy Systems*, vol. 71, pp. 242–253, 2015.

[27] C. Zhang, T. Liu, and T. Bu, "Dynamic optimal dispatch of wind-hydro-thermal power system," *Modern Electric Power*, vol. 34, no. 04, pp. 8–14, 2017.

[28] S. Dehghan, N. Amjady, and A. Kazemi, "Two-stage robust generation expansion planning: A mixed integer linear programming model," *IEEE Transactions on Power Systems*, vol. 29, no. 2, pp. 584–597, 2014.

[29] H. Gao, J. Liu, Z. Wei, and Y. Su, "A bi-level robust planning model of active distribution network and its solution method," *Proceedings of the Chinese Society of Electrical Engineering*, vol. 37, no. 5, pp. 1389–1400, 2017.

[30] X. Wu, X. Wang, J. Wang et al., "Economic generation scheduling of a microgrid using mixed integer programming," *Proceedings of the CSEE*, vol. 33, no. 28, pp. 1–9, 2013.

[31] S. Surender Reddy, J. Y. Park, and C. M. Jung, "Optimal operation of microgrid using hybrid differential evolution and harmony search algorithm," *Frontiers in Energy*, vol. 10, no. 3, pp. 355–362, 2016.